

Right is not always wrong: DTI and fMRI evidence for the reliance of reading comprehension on language-comprehension networks in the right hemisphere

Tzipi Horowitz-Kraus · Molly Grainger ·
Mark DiFrancesco · Jennifer Vannest · Scott K. Holland ·
CMIND Authorship Consortium

Published online: 17 December 2014
© Springer Science+Business Media New York 2014

Abstract The Simple View theory suggests that reading comprehension relies on automatic recognition of words combined with language comprehension. The goal of the current study was to examine the structural and functional connectivity in networks supporting reading comprehension and their relationship with language comprehension within 7-9 year old children using Diffusion Tensor Imaging (DTI) and fMRI during a Sentence Picture Matching task. Fractional

Anisotropy (FA) values in the left and right Inferior Longitudinal Fasciculus (ILF) and Superior Longitudinal Fasciculus (SLF), known language-related tracts, were correlated from DTI data with scores from the Woodcock-Johnson III (WJ-III) Passage Comprehension sub-test. Brodmann areas most proximal to white-matter regions with significant correlation to Passage Comprehension scores were chosen as Regions-of-Interest (ROIs) and used as seeds in a functional connectivity

The CMIND (Cincinnati MR Imaging of NeuroDevelopment) Authorship Consortium

Scott K. Holland, PhD^{1,6,9,10}
Jennifer Vannest, PhD^{1,5}
Vincent J. Schmithorst, PhD^{1,2}
Mekibib Altaye, PhD^{1,7}
Gregory Lee, PhD^{1,6}
Luis Hernandez-Garcia, PhD³
Michael Wagner, PhD^{1,8}
Arthur Toga, PhD^{12,13}
Jennifer Levitt, MD¹⁴
Anna W. Byars, PhD^{1,5}
Andrew Dimitrijevic, PhD^{9,10}
Nicolas Felicelli⁸
Darren Kadis, PhD^{1,5}
James Leach, MD^{1,6}
Katrina Peariso, MD, PhD⁵
Elena Plante, PhD⁴
Akila Rajagopal, MS¹
Andrew Rupert, MS⁸
Mark Schapiro, MD^{1,5}
Ronald Ly¹⁴
Petros Petrosyan¹²
JJ Wang, PhD¹¹
Lisa Freund, PhD¹⁵

¹Pediatric Neuroimaging Research Consortium, Cincinnati Children's Hospital Medical Center, University of Cincinnati, Cincinnati, OH

²Pediatric Imaging Research Center, Dept. of Radiology, Children's Hospital of Pittsburgh of UPMC, Pittsburgh, PA

³Functional MRI Laboratory, Dept. of Biomedical Engineering, University of Michigan, Ann Arbor, MI

⁴Dept. of Speech, Language, and Hearing Sciences, University of Arizona, Tucson, AZ

⁵Div. of Neurology, Dept. of Pediatrics, Cincinnati Children's Hospital Medical Center, University of Cincinnati, Cincinnati, OH

⁶Dept. of Radiology, Cincinnati Children's Hospital Medical Center, University of Cincinnati, Cincinnati, OH

⁷Div. of Biostatistics and Epidemiology, Dept. of Pediatrics, Cincinnati Children's Hospital Medical Center, University of Cincinnati, Cincinnati, OH

⁸Div. of Biomedical Informatics, Dept. of Pediatrics, Cincinnati Children's Hospital Medical Center, University of Cincinnati, Cincinnati, OH

⁹Dept. of Otolaryngology, Cincinnati Children's Hospital Medical Center, University of Cincinnati, Cincinnati, OH

¹⁰Communication Sciences Research Center, Cincinnati Children's Hospital Medical Center, University of Cincinnati, Cincinnati, OH

¹¹Dept. of Neurology, UCLA, Los Angeles, CA

¹²Laboratory of Neuroimaging, Keck School of Medicine of USC, Los Angeles, CA

¹³Departments of Ophthalmology, Neurology, Psychiatry, and the Behavioral Sciences, Radiology and Engineering, Keck School of Medicine of USC, Los Angeles, CA

¹⁴Psychiatry and Biobehavioral Sciences, UCLA, Los Angeles, CA

¹⁵Eunice Kennedy Shriver National Institute of Child Health and Human Development, Bethesda, MD

T. Horowitz-Kraus (✉) · M. Grainger · M. DiFrancesco ·
J. Vannest · S. K. Holland

Pediatric Neuroimaging Research Consortium, Cincinnati Children's Hospital Medical Center, University of Cincinnati, Cincinnati, OH, USA

e-mail: Tzipi.Horowitz-Kraus@cchmc.org

analysis using the Sentence Picture Matching task. The correlation between percentile scores for the WJ-III Passage Comprehension subtest and the FA values in the right and left ILF and SLF indicated positive correlation in language-related ROIs, with greater distribution in the right hemisphere, which in turn showed strong connectivity in the fMRI data from the Sentence Picture Matching task. These results support the participation of the right hemisphere in reading comprehension and may provide physiologic support for a distinction between different types of reading comprehension deficits vs difficulties in technical reading.

Keywords Children · Diffusion tensor imaging · fMRI · Language · Reading · Reading comprehension · Right hemisphere · Semantic

Introduction

Reading comprehension is defined as a gained understanding of written text through the process of extracting and constructing meaning (Rimrodt et al. 2009), and is one of the most essential academic skills (Nation and Snowling 1997). In the United States alone, 10–15 % of school-age children exhibit poor comprehension skills despite normal levels of reading accuracy and fluency (Stothard and Hulme 1995; Yuill and Oakhill 1991). The Simple View theory of reading suggests that reading comprehension relies on both technical reading (decoding and word recognition) and language comprehension (Gough and Tunmer 1986). However, it is challenging to isolate the mechanisms underlying reading comprehension (Spencer et al. 2014). The current study used neuroimaging tools to identify associations between reading comprehension and more basic linguistic abilities.

Prior imaging studies of reading comprehension have largely focused on word- or sentence-level processing (Booth et al. 1999; Caplan et al. 2001; Cutting et al. 2006; Keller et al. 2003; Mason and Just 2007; Meyer et al. 2000; Ni et al. 2000; Rimrodt et al. 2009). In general, reading sentences activates the same regions as reading words with more widespread and bilateral activation, specifically in the middle and superior temporal gyri, bilateral temporal poles, and left frontal and parietal regions. A recent study using Diffusion Tensor Imaging (DTI) data enabled the distinction between reading comprehension and technical/orthographic reading by demonstrating that these abilities are associated with two distinct white matter tracts (Horowitz-Kraus et al. 2014), which was done by correlating the white matter integrity (defined by Fractional Anisotropy; FA) with reading measures. The FA values in the left Arcuate Fasciculus [AF, a part of the Superior Longitudinal Fasciculus (SLF)] were correlated with greater reading scores (from the TOWRE-2 test; Torgesen et al. 2012), whereas the FA values in the right Inferior Longitudinal

Fasciculus (ILF) were correlated with Passage Comprehension scores (from the Woodcock-Johnson III or WJ-III battery; see Woodcock et al. 2001). The results of that study also provided additional support for the role of the right hemisphere in reading/language comprehension. This view is supported by the different subpopulations of individuals with difficulties in reading comprehension: those who have impaired technical reading vs those who have intact technical reading, but other language problems (see Spencer et al. 2014). Studies in which participants were asked to comprehend auditory-presented narrative (listen to stories) reported larger regions of right temporal lobe activity than when participants listened to the same sentences presented in a conceptually unrelated manner (e.g., Plante et al. 2006; Robertson et al. 2000). These studies raise the question of precisely which language-comprehension skills the right hemisphere might support.

Evidence from patients with right hemisphere brain damage suggests that these patients demonstrate deficits comprehending nonliteral and indirect language including metaphors, humor, and sarcasm (e.g., see Johns et al. 2008 for a review). Despite evidence of understanding the main ideas contained in a narrative, these patients also were unable to use semantic context to interpret new information (Roman et al. 1987; Wapner et al. 1981). These findings raise the question as to the relationship between reading comprehension and neural circuits supporting language comprehension.

Semantics is one of the first stages in language comprehension (Friederici 2012; Muller and Hagoort 2006). Ventral and dorsal pathways have been shown to have a role in language comprehension (Friederici 2012). The ventral pathway supports semantic and syntactic processes and connects the temporal cortex with Broca's area [Brodmann area (BA) 44] through two white matter tracts: the AF and the ILF. The dorsal pathway is involved in syntactic processes and connects the temporal cortex with premotor cortex through the parts of the SLF not including the AF (see Friederici 2012 for the complete model). Despite the knowledge of the involvement of the Superior Temporal Gyrus (STG; BA22), frontal operculum (BA 44), pars opercularis (BA 45) and the triangularis pars orbitalis (BA 47) in semantic processing, the exact neural circuits supporting semantic processing and how this ability corresponds with reading comprehension are still a matter of debate (Friederici et al. 2006; 2012).

The current gap in understanding of the Simple View theory is the lack of functional and anatomical evidence supporting the reliance of reading comprehension on neural circuits supporting language comprehension. Obtaining this information would provide biological support for the Simple View theory as well as for impairments, including for individuals who suffer from reading comprehension problems despite intact reading proficiency (for further description of this population, see Spencer et al. 2014). The

purpose of the current study was to examine the structural connectivity in networks supporting reading comprehension using DTI data and its relationship to functional connectivity in a language comprehension fMRI task.

Since sentence processing is considered a language comprehension task that encompasses semantic and syntactic components as in reading comprehension, we examined the shared neural circuits between reading and language comprehension as measured by the percentile for the Passage Comprehension test (from WJ-III; Woodcock et al. 2001) and a Sentence Picture Matching functional magnetic resonance imaging (fMRI) task in 7–9 year old children using DTI. This age range was selected because children were part of a larger longitudinal study that enabled us to collect the WJ-III Passage Comprehension percentiles from them in the final year of scanning and testing. This is an interesting age range because during this developmental period, children are transitioning from the stage of “learning to read” to “reading to learn” (Chall 1983). Namely, they master technical reading and start developing reading comprehension skills (Chall 1983). So we expect to see the emergence of right hemisphere comprehension abilities, activity, and connectivity. We hypothesized that Regions of Interest (ROIs) resulting from the voxel-wise correlation of DTI white matter FA (focusing on the dorsal pathway, SLF and the ventral pathway, ILF) with reading comprehension measures (i.e., percentiles from the Passage Comprehension task) also would be part of the activation observed in response to the fMRI Sentence Picture Matching task. We also hypothesized that in addition to the involvement of the right hemisphere in the Sentence Picture Matching task, ROIs related to reading comprehension would show greater functional connectivity in the right hemisphere as compared to the homologous ROIs in the left hemisphere.

Methods

Participants

Twenty three healthy children (8.5 ± 0.81 years old, 8 males) participated in the current study. All children were right-handed with an average to above average IQ (107.81 ± 13.84) as measured by the Wechsler Intelligence Scale for Children (WISC-IV) test (Wechsler 2003).

Behavioral measures

Reading comprehension was measured using the Passage Comprehension subtest from the WJ-III (Woodcock et al. 2001). In this test, participants are required to read a sentence or paragraph and supply a missing word that is implied by the context of the text. Within the range of 7–9 years of age, typical readers may demonstrate different levels of reading

comprehension skills (see Chall’s model for reading acquisition; Chall 1983). To compare the level of age-appropriate reading comprehension skills across all participants, we calculated the percentiles for the Passage Comprehension subtest based on the age norms from the WJ-III battery. An independent *t*-test analysis revealed no significant difference between boys and girls in Passage Comprehension percentiles ($t(21) = -0.034$, $P > 0.05$).

Imaging data - diffusion tensor imaging data acquisition and processing

DTI data were acquired using single-shot spin-echo, echo planar imaging with TR/TE=8800/88 ms, 61 gradient directions, and b-value of 1000 s/mm^2 . Images were pre-processed in FSL (FMRIB, Oxford, UK) including correction for eddy currents and head motion. Tensor decomposition was done using FDT (FMRIB’s Diffusion Toolbox) (Behrens et al. 2003) for generating FA indices. Tract-Based Spatial Statistics (TBSS) (Smith et al. 2006) was then used to prepare the individual diffusion maps for voxel-based group analysis by performing the following steps: all FA images were nonlinearly registered to a template of averaged FA images (FMRIB-58) in Montreal Neurological Institute (MNI) space with 1 mm resolution using FNIRT (FMRIB, Oxford, UK). It has been shown previously that the MNI adult framework is adequate for co-registration of DTI data from adolescent and child brains (Wilke et al. 2003; Wang et al. 2012).

After transformation into MNI space, a cohort mean-FA image was created and thinned to generate a cohort mean-FA skeleton of the white matter tracts. Each subject’s aligned FA image was then projected onto the cohort mean-FA skeleton by filling that with FA values from the nearest relevant tract center, which was achieved by searching perpendicular to the local skeleton structure for maximum value. A second localized co-registration step helped alleviate alignment problems (see Fig. 1 for this procedure). Then, two white matter tracts, ILF and SLF, were defined as ROIs to further constrain the voxel-wise TBSS analysis in these two tracts in each hemisphere (Yeatman et al. 2012) (see Fig. 2 for the ILF and SLF masks).

Statistical analysis for the DTI correlation with the percentiles for the passage comprehension subtest

After the projection of each subject’s FA skeleton to the group mean-FA skeleton and following the second co-registration, we correlated the mean FA measures from these ROIs from each individual with the percentiles for the Passage Comprehension subtest from WJ-III. On a voxel-wise basis within each ROI, correlation of FA with percentiles for the Passage Comprehension subtest was measured and tested for statistical significance by a non-parametric permutation-based method

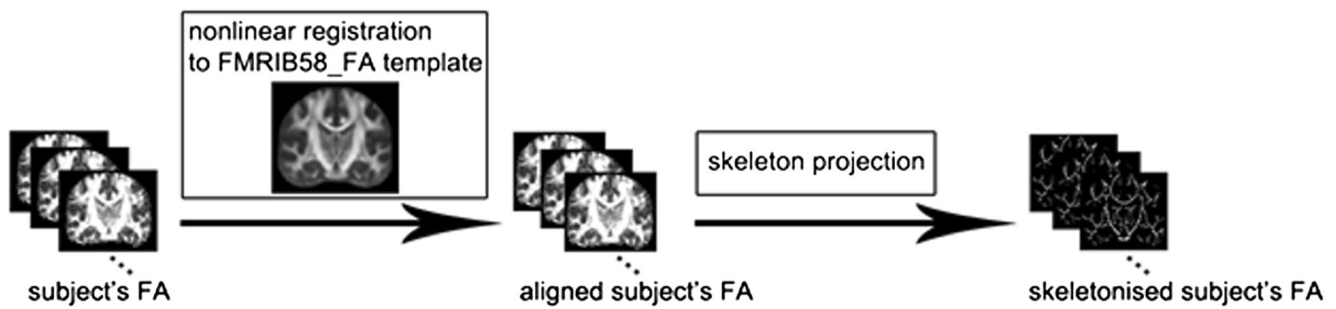


Fig. 1 The TBSS pipeline

provided by the RANDOMIZE algorithm (Nichols and Holmes 2002) using 5000 permutations with Threshold-Free

Cluster Enhancement (TFCE) (Smith et al. 2007). Using the Harvard-Oxford atlas implemented in FSL, we extracted the nearest grey matter point (and the corresponding BA) for each cluster found in the ILF and SLF ROI that reached a significance level of $P < 0.005$, uncorrected for multiple comparisons among voxels. These Brodmann areas were then used as ROIs in functional connectivity analysis of fMRI data acquired during a Sentence Picture Matching task. It is important to note that each BA ROI in the functional connectivity analysis may correspond to multiple proximal DTI sub-clusters.

Functional MRI sentence picture matching task

Five cycles of alternating blocks of sentences and words (64 s per block) were presented for a total scan time of 10 min 40 s; 10 blocks overall. The “stimulated” condition of the sentences involved auditory presentation of a simple active or passive sentence simultaneously with visual presentation of a picture of two objects either acting on each other (e.g., “the dog is licking the cat”) or in a spatial relationship (e.g., “the book is on the table”). During the control condition, single nouns were presented auditorily and repeated four times so that noun stimuli were similar in duration to sentence stimuli, and a picture of a single object was presented (designed to occupy roughly the same degree of the visual field as the two-object pictures). Participants were asked, for both conditions, to make a button-press response indicating if the auditory stimulus accurately described the picture. Each block included 15 trials (4250 ms each), and these blocks were counterbalanced for yes/no responses and sentence type. See Fig. 3 for task details. The participants’ behavioral responses were recorded, and performance scores (i.e., the percentage of correct responses) were calculated in order to ensure that the task was understood.

Functional MRI data acquisition and processing

Data for the Sentence Picture Matching task was acquired using a combined Whole-Brain Functional ASL/BOLD Gradient-Echo EPI Acquisition. MRI data was obtained using a Philips 3 T Achieva system and a 32-channel head coil. For the ASL/BOLD acquisitions, a double-excitation approach was used, which has been determined both theoretically and

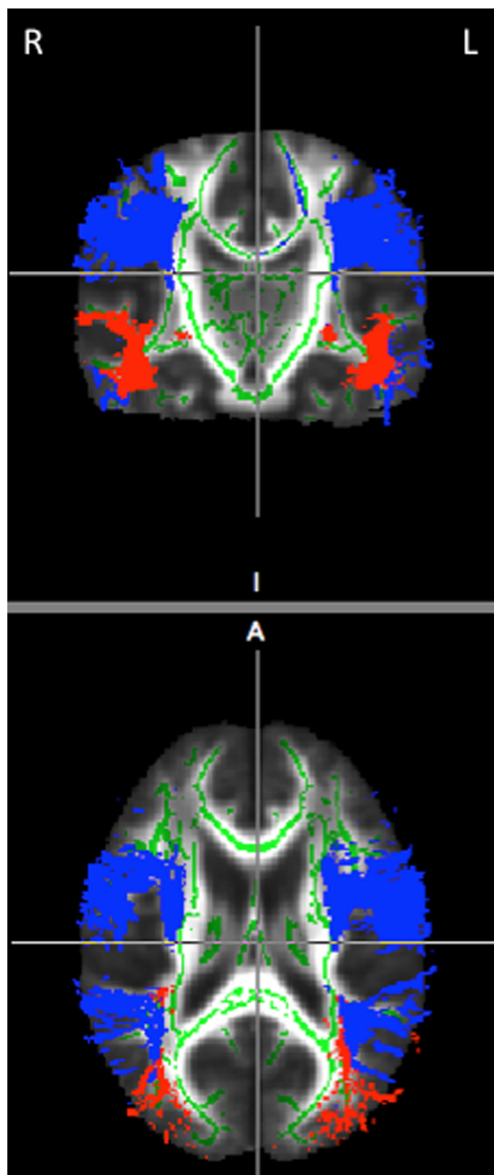
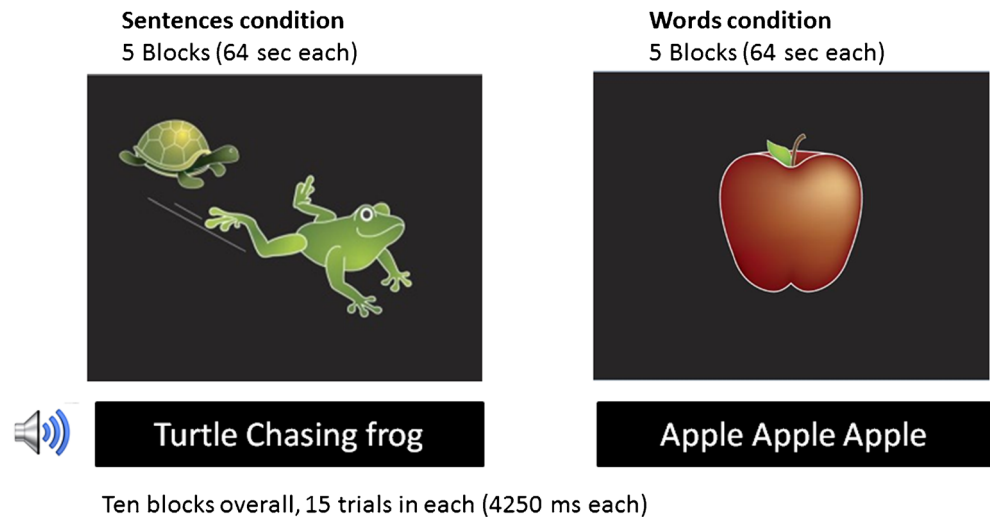


Fig. 2 Masks for the right and left ILF (red) and SLF (blue). Masks for the right and left ILF (red) and SLF (blue). The masks were created based on the JHU white matter tractography atlas. Masks presented in radiological orientation (L=R/R=L)

Fig. 3 The functional MRI Semantic task



empirically to be more optimal as compared to double-echo acquisitions or other methods (Schmithorst et al. 2014). However, only standard BOLD acquisitions were included in the present analysis. Acquisition parameters were: TR=4000 ms, TE1=11 ms, TE2=35 ms, matrix=64×64, FOV=25.6×25.6 cm, slice thickness=5 mm, 25 slices acquired covering the whole brain.

Participants were acclimated and desensitized to the scanner (see Byars et al. 2002 and Vannest et al. in press). Prior to study visits and in order to prepare the child for the study visit, the parents and child watched a video describing the MRI as an adventure in space. This video is available on our project website <https://research.cchmc.org/c-mind/visitors/preparing>. Specific procedures were used at each visit to acclimate the child to the scanner environment. Before the scanning session, children practiced the tasks in a mock scanner that included scanner sounds. Children also were offered to move the actual scanner bed up and down and to sit on the bed. Tasks were practiced both on a computer outside of the scanner as well as inside the scanner before image acquisition. Children were introduced with a framed picture of a scanned brain during motion as compared to a framed picture of a scanned brain where the participant was lying still. They also practiced a position of “lying still as a statue” within the scanner (meaning, lying still without moving their head, legs, and arms). Head motion was further minimized using elastic straps that were attached to either side of the head-coil apparatus.

Functional MRI data analysis

First-level fMRI data processing was carried out using FEAT (fMRI Expert Analysis Tool) Version 6.0, which is a part of FSL (FMRIB’s Software Library, www.fmrib.ox.ac.uk/fsl) involving motion correction, spatial smoothing, and coregistration to an age-appropriate pediatric template

(template for 4–18 year olds, for details see: https://research.cchmc.org/c-mind-db/py-doc/html/pipelines_struct.html#registration-to-the-study-template) that was then normalized to 2 mm MNI standard space using symmetric diffeomorphic image normalization (SyN) (Avants et al. 2008) as implemented in ANTs (Advanced Normalization Tools, stnava.github.io/ANTs/). Independent motion correction of the ASL and BOLD time series (to a common reference frame) was carried out using MCFLIRT (Jenkinson et al. 2002). In an initial run, the central time point was used as the reference frame. Based on the derived motion parameters, the time point with the minimal displacement from the average position of the brain over the time series was determined. Motion correction was then restarted, using this minimal displacement time point as the reference frame. Following motion correction, spatial smoothing using a Gaussian kernel of FWHM 8 mm and high-pass temporal filtering (cutoff of 104 s) were applied. Grand-mean intensity normalization by a single multiplicative factor was applied to each 4D dataset.

To verify involvement of the right hemisphere in the Sentence Picture Matching task even in the absence of a priori selection of ROIs (i.e., for a whole-brain analysis), a general linear model analysis was performed. A general linear model with autocorrelation correction was used to compute BOLD and ASL activation at the single-subject level. For the present analysis, only BOLD data was considered (comparison with ASL is beyond the scope of this paper – See Schmithorst et al. 2014). Sentences and words conditions were then modeled and parameter maps were generated for the contrast between sentences and words (sentences>words).

For the second-level analysis, group-level analyses were carried out using a random-effects ordinary least-squares model. To control for the percentage of false-positive active voxels within each activated cluster, we employed a False Discovery Rate (FDR) correction with a threshold of $P<0.05$ (also see Benjamini and Hochberg 1995). Since the

current study focuses on comprehension beyond the single-word level, our analysis was focused only on the sentences > words contrast.

Functional connectivity analysis

Our regions of interest for functional connectivity analysis were selected by first locating the nearest grey matter points to the white matter regions (in the right and left ILF and SLF) where FA was significantly correlated with percentile scores for the Passage Comprehension subtest. Then, we chose the Brodmann Areas where these grey matter points were located as ROIs, for functional connectivity analysis (see also *Statistical analysis for the DTI correlation with the percentiles for the Passage Comprehension subtest*). To represent the linear temporal association between the ROIs, bivariate regression coefficient values were estimated using the CONN fMRI connectivity toolbox in SPM8 (v14, <http://www.nitrc.org/projects/conn>; Whitfield-Gabrieli and Nieto-Castanon 2012). This toolbox implements a component-based noise correction method (CompCor) for reducing physiological and other nuisance effects (i.e., white matter and CSF effects, sentence and word tasks' effects and their first temporal derivatives, and motion effects), allowing group inferences to be made using random effects in a second-level analysis. Bivariate correlation (i.e., connectivity) from the sentences condition for each participant was correlated with the

participant's performance score during the task (i.e., the overall performance percentage that reflects whether the participant provided a correct or erroneous response during the task), such that the correlation coefficients (β) represent a performance weighted within-group measure of functional connectivity between ROIs. Only connections that survived the significance threshold for functional connectivity and behavioral measures were included in the results ($P < 0.0005$ FDR-corrected, two-sided; see Benjamini and Hochberg 1995). An intensity value for each ROI was defined as the number of significant connections made to all other ROIs (representing the degree of connectivity).

Results

Behavioral measures

Reading comprehension scores (from the Passage Comprehension subtest) Average percentile for the Passage Comprehension WJ-III: 50.87 % ± 22.36 %.

Behavioral scores for the Sentence Picture Matching task (performance scores) Results from the average correct responses for the sentences condition showed 86.0 % ± 10.7 % accuracy.

Table 1 Regions within the ILF and SLF corresponding with the correlation between FA values and Passage Comprehension scores ($P < 0.005$, uncorrected). Regions were defined using the Harvard-Oxford atlas in FSL. Coordinates are reported in MNI space

Tract	Nearest-point grey-matter functional region using the Talarach-Daemon Atlas	For visual demonstration of the regions, see Figure #	Corresponding BAs	Cluster size (voxels)	Cluster coordinates (x, y, z)
R ILF	Lateral occipital cortex	4A	19	9	50, 52, 76
	Heschl's gyrus, superior temporal gyrus	4A	41, 22	19, 21	42, 115, 65, 42, 106, 74
	Superior temporal gyrus, frontal opercular cortex	4B	22, 47	2	31, 116, 73
L ILF	Occipital fusiform gyrus, lateral occipital gyrus, temporal occipital fusiform gyrus	4B	37, 19	10	
	Inferior temporal gyrus, temporal fusiform gyrus, inferior temporal gyrus	4B	20, 37	10	134, 89, 54
	Precuneous, lateral occipital gyrus, cuneal gyrus	4B	7, 19, 18	1	99, 53, 62
R SLF	Inferior temporal gyrus, middle temporal gyrus, temporal fusiform gyrus	4A	20, 21	1	35, 96, 52
	Parietal operculum, supramarginal gyrus, postcentral gyrus	4A	40, 6, 43	1	44, 100, 97
	Middle frontal gyrus	4A	46	4	77, 122, 119
	Superior frontal gyrus	4A	10	6	78, 145, 126
L SLF	Superior frontal gyrus	4B	10	5	104, 147, 118
	Superior temporal gyrus, Heschl's gyrus	4B	41, 22	2	137, 104, 72

ILF Inferior Longitudinal Fasciculus, SLF Superior Longitudinal Fasciculus, FA Fractional Anisotropy

Imaging measures

Diffusion tensor imaging measures

Clusters of white matter voxels in the right and left ILF and SLF with moderate positive correlation between the FA values and the percentiles for the Passage Comprehension subtest were found ($P < 0.005$, uncorrected). Percentiles for Passage Comprehension were positively correlated with FA values in both the right and left ILF and SLF. See Table 1 and Fig. 4 for more information.

General linear model for the sentence picture matching task

The composite map for the fMRI task reveals activation clusters within key language regions as listed in Table 1 (left and right frontal poles, inferior frontal gyri, middle temporal gyri, angular gyri, and fusiform gyri; $P < 0.05$, FDR-

corrected). See Fig. 5 for the activation of the sentences > words contrast and Table 2 for these regions.

Functional connectivity for the sentence picture matching task

Based on the clusters found in the correlation of the percentiles for the Passage Comprehension subtest with the FA values in the selected white matter tract ROIs, 19 ROIs were included in the functional connectivity analysis (11 ROIs in the right hemisphere and 8 ROIs in the left hemisphere). Participants showed significant positive performance-related functional connectivity between the chosen ROIs, at $P < 0.0005$, FDR corrected. A trend of greater intensity values for right lateralized ROIs compared to the intensity of their left homologues was observed. Despite this trend, a paired *t*-test analysis comparing the intensity of ROIs that had homologous ROIs (i.e., BAs 10, 19, 22, 41) did not reveal a statistically significant difference ($P > .05$). See Fig. 6 and Table 3 for details.

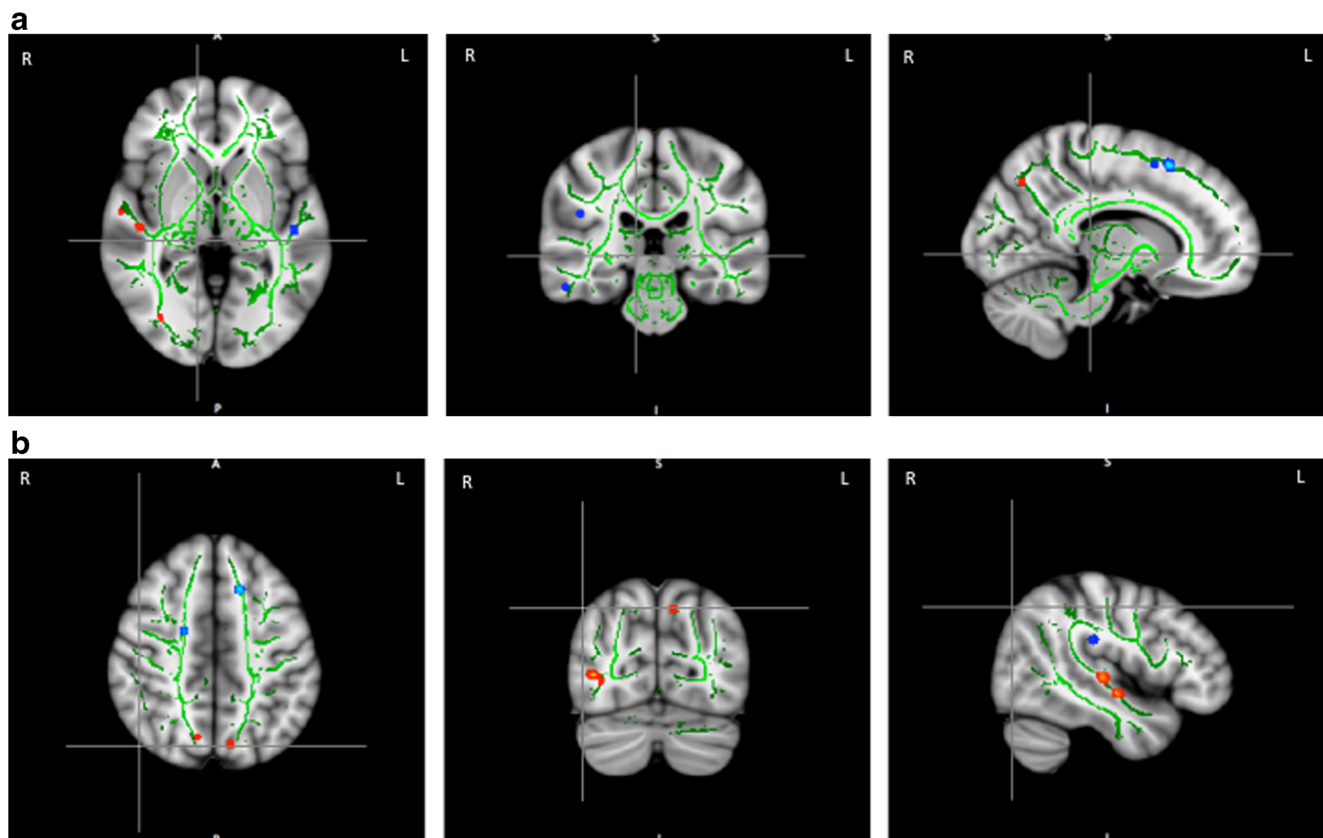


Fig. 4 Illustration of the major correlation between the FA values right and left in SLF and ILF with the percentiles for the Passage Comprehension task. Right and left ILF (red) and SLF (blue). Tracts were defined based on the JHU white matter atlas. Data is presented in Radiological orientation (L=R/R=L). **a** Three dimensional tractography results demonstrating right lateralization of correlation of FA values with percentiles for the Passage Comprehension subtest ($P < .005$,

uncorrected). Axial, coronal, and sagittal views are shown at MNI coordinates $x=12, y=-28, z=0$. **b** Three dimensional tractography results demonstrating right lateralization of correlation of FA values with percentiles for the Passage Comprehension subtest ($P < .005$, uncorrected). Axial, coronal, and sagittal views are shown at MNI coordinates $x=47, y=-74, z=44$

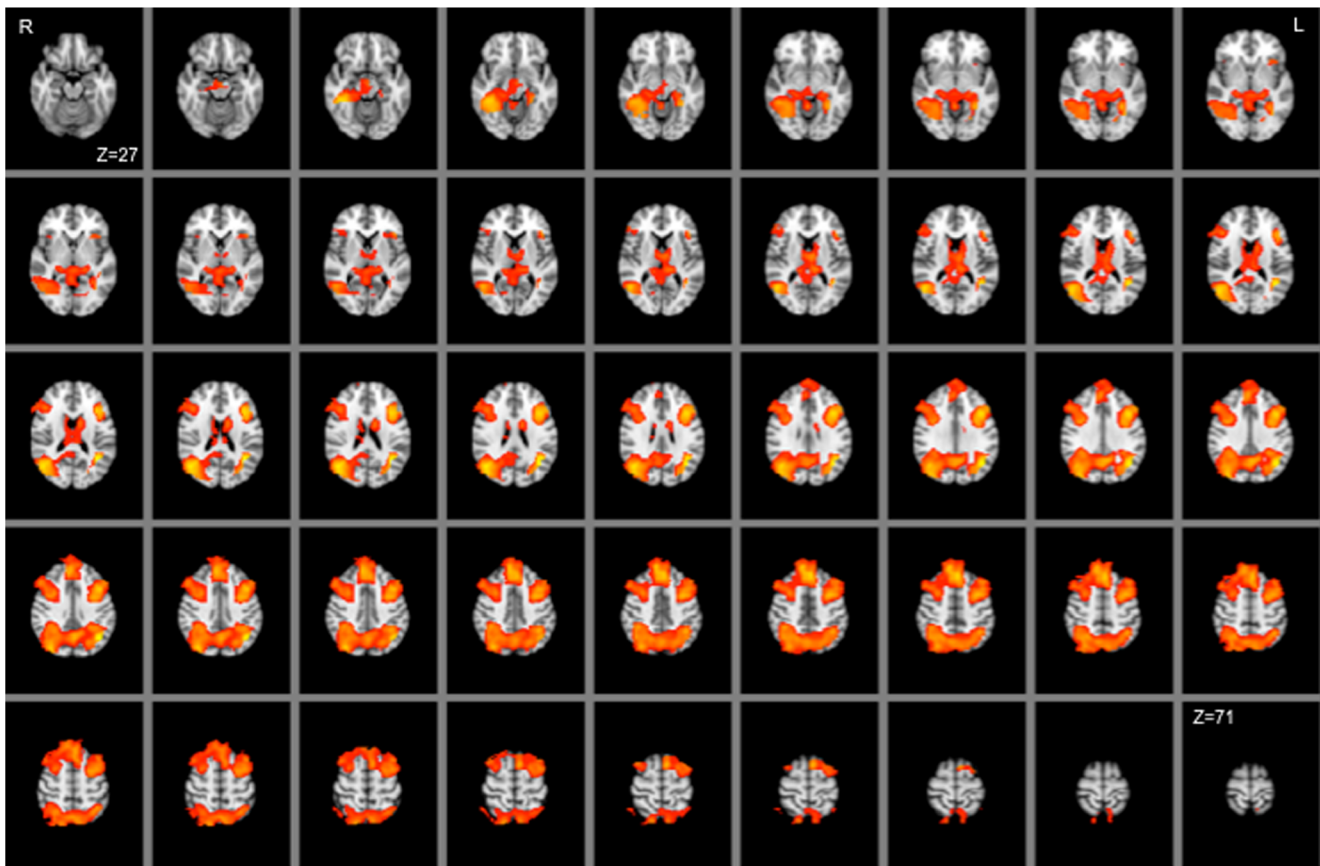


Fig. 5 GLM analysis for the Sentence Picture Matching task (sentences>words). GLM second-level analysis (sentences>words), $P < 0.05$, FDR-corrected ($Z = 2.3\text{--}6.2$), Data presented in radiological

orientation (R=L, L=R). The red color represents the data for sentences>words contrast. Slices shown are $Z = 27\text{--}71$

Discussion

The purpose of the current study was to provide neurobiological support for the utilization of the right hemisphere in reading comprehension through the use of structural and functional connectivity. Our results indicate a significant correlation of FA values in SLF and ILF with the percentiles for the Passage Comprehension subtest from WJ-III, and with a greater distribution in the right hemisphere, which adds an interesting laterality aspect to the Freiderici model (2012). While the GLM maps for the Sentence Picture Matching task fMRI task showed a bilateral activation in language-related regions during the sentence processing vs words contrast, the functional connectivity results showed a trend of greater intensity for right-lateralized ROIs as compared to the left homologues. This is a novel and important finding guided by the underlying white matter structure defined by the DTI results correlating the FA values from the chosen white matter tracts (right and left ILF and SLF) with the percentiles for the Passage Comprehension subtest from the WJ-III.

The results of our study confirm the hypothesis that reading comprehension relies mainly on the right hemisphere, even in children as young as 7–9 years of age. This is reflected by the

significant correlation we determined between FA values in SLF and ILF and the percentiles for the Passage Comprehension subtest, specifically in the right hemisphere. These results are in line with our previous analysis in adolescents ages 15 to 19 (Horowitz-Kraus et al. 2014). Using TBSS voxel-wise analysis, we demonstrated positive correlations between regional FA values in the right and left Arcuate Fasciculus (AF) and the percentiles for the Passage Comprehension subtest, with a robust correlation in the right hemisphere. A left-lateralized correlation between the ILF and a word recognition measure [the Test of Word Recognition (i.e., TOWRE-2; Torgesen et al. 2012)] also was previously found (Horowitz-Kraus et al. 2014). There, we suggested that the AF supports reading comprehension due to its wide distribution among reading-related regions (see Yeatman et al. 2012). Regions of the right frontal lobe connected to posterior temporal parietal language areas are an inherent part of an effective reading comprehension circuit in typical reading, and are connected through the AF (Horowitz-Kraus et al. 2014). In the current study, we demonstrated a significant correlation of percentile score for the Passage Comprehension test with FA values in specific other parts of the right SLF. Previous studies have shown that the AF is the last

Table 2 Coordinates, Brodmann areas and cluster sizes for the second-level analysis for the Sentence Picture Matching task (sentences>words), $P<0.05$ -FDR corrected. x, y, and z coordinates correspond to the center of each cluster. Regions were defined using the Harvard-Oxford atlas in FSL

Location	# of voxels	BA	X	Y	Z
Right lateral occipital gyrus ^a	4683	18/19	34	-70	36
Right precuneous ^a	3375	7	2	-62	40
Right frontal pole	1642	10	6	52	42
Right angular gyrus	986	39	44	-54	30
Right middle temporal gyrus	735	21	52	-52	2
Right superior parietal gyrus	689	7	30	-48	46
Right lingual gyrus ^a	644	19	20	-50	-4
Right paracingulate gyrus	591	24	2	32	38
Right inferior lateral occipital gyrus	584	18	44	-64	6
Right pars triangularis	475	45	48	28	14
Right parahippocampal gyrus	397	27/34/35	22	-32	-10
Right precentral gyrus	350	4/6	38	4	32
Right temporal occipital fusiform gyrus	319	37	34	-50	-10
Right inferior temporal gyrus ^a	303	20	46	-50	-8
Right inferior frontal gyrus	287	9/5/44/46	44	16	24
Right occipital fusiform gyrus	160	37	32	-66	-6
Left lateral occipital gyrus ^a	2429	18/19	-24	-68	44
Left superior frontal gyrus ^a	3292	6/8/9	0	28	50
Left middle frontal gyrus ^a	3224	6/8/9/10	-38	14	42
Left precentral gyrus	662	4/6	-38	2	34
Left superior parietal gyrus	659	7	-30	-52	46
Left angular gyrus	552	39	-40	-56	32
Left inferior frontal gyrus	486	9/5/44/46	-42	16	22
Left parahippocampal gyrus	306	27/34/35	-22	-34	-8
Left insular cortex	92	13	-32	18	0
Left frontal operculum ^a	89	44	-40	22	4
Left temporal occipital fusiform cortex ^a	66	37	-38	-52	-6
Left middle temporal gyrus	28	21	-38	-52	14

^a Indicates those regions that also were shown to be significant in the DTI analysis

white matter tract supporting language to myelinate (Su et al. 2008), which may explain the absence of a significant correlation in the current study since it included relatively young children (7–9 years in the current analysis vs 15–19 years in Horowitz-Kraus et al. 2014). However, our results do confirm that the role of the right hemisphere in reading comprehension begins as early in life as at the age of 7. Interestingly, it seems that the utilization of the right hemisphere for reading comprehension continues into late adolescence, while engaging different brain regions as well as extending the connections between reading regions in the right hemisphere also occur in 15–19 year-old children (Horowitz-Kraus et al. 2014). A future longitudinal study comparing the correlation between FA values and percentile scores for the Passage Comprehension test across development should verify this point.

Interestingly, in contrast to the trend of greater functional connectivity values in the majority of the right ROIs vs the left ROIs in the functional connectivity analysis, BA 19 showed a

trend of greater intensity in the left hemisphere rather than in the right (118.64 vs 109.57, respectively). Two other closely related regions showed significant functional connectivity only in the left hemisphere: left BAs 18 and 37 as well as left BA 7. Interestingly, these regions in the left hemisphere are key elements of the ventral occipito-temporal stream, also known as the Visual Word-Form Area (VWFA; see Turkeltaub et al. 2003). A future study should verify if the role of the left BAs 18, 19 and 37 in reading comprehension may be due to the technical reading component in reading comprehension. Moreover, the role of left BA 7 was thought to be related to visual attention, which is a crucial component in technical reading (Vogel et al. 2014). A future study should specifically examine the functional connectivity of the left BAs 18, 19, 37 and 7 with regions related to technical reading and reading comprehension in the right hemisphere to reveal the role of the left hemisphere in comprehension rather than in technical reading.

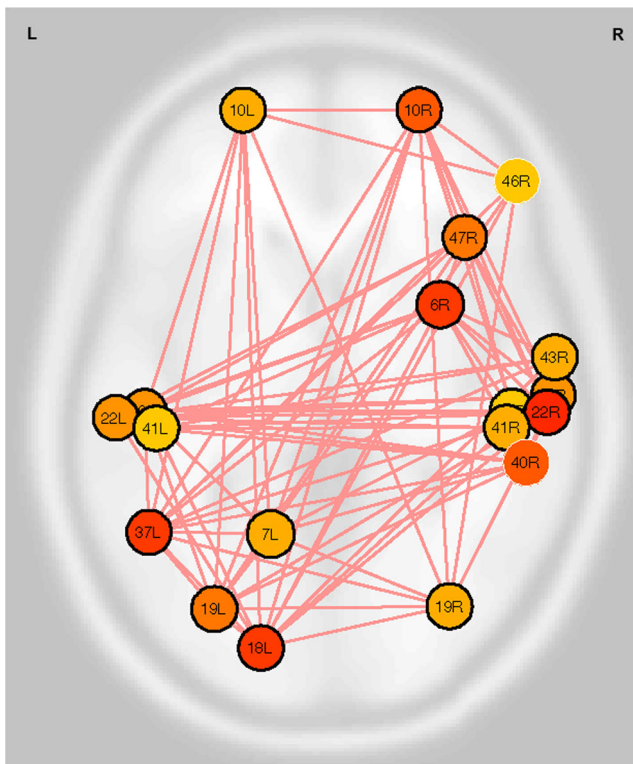


Fig. 6 Functional connectivity between the selected ROIs for the sentences condition. Highest functional connectivity (strongest connections >10) is colored in red, mild in orange, lowest in yellow (<5 connections), $P < 0.0005$, FDR-corrected. Data presented in neurological orientation (R = R, L = L). ROIs were defined based on the Talairach-Daemon atlas implemented in the CONN toolbox

The group random-effects GLM analysis for sentences contrasted with words in the Sentence Picture Matching task (Fig. 5) shows bilateral activation of language regions, whereas the functional connectivity base showed a trend of greater right lateralization. This likely is due to the involvement of additional language processes for comprehension as well as syntactic and semantic processing while participating in the Sentence Picture Matching task. Bilateral activation in the STG previously has been observed in adults in response to semantically and syntactically violated sentences (Friederici et al. 2003) as well as during a narrative comprehension task along development (Horowitz-Kraus et al. 2013). The fMRI task used in the current study involved a semantic and syntactic decision through an auditory processing pathway that tends to engage bilateral activation. Our data support the bilateral utilization of two white matter tracts underlies the STG (SLF, ILF) associated with percentiles for the Passage Comprehension subtest. The bilateral activation of the STG and the frontal operculum during the Sentence Picture Matching task was also observed in the GLM analyses. However, no significant connectivity in the pars opercularis or other regions of the inferior frontal gyrus (IFG) was found for the Sentence Picture Matching task. Combining the absence of this finding in comparison with our previous study

(Horowitz-Kraus et al. 2014) suggests that the most frontal regions of the SLF are not utilized in language comprehension by younger children. The significant correlation of the middle temporal gyrus (MTG), the angular gyrus (AG), and the orbitofrontal cortex (oPFC) with Passage Comprehension scores, as well as the evidenced connectivity of these regions during the fMRI task, corresponds with previous reports of activation of these regions in sentence processing (Friederici 2009).

Conclusions

The current study strengthens the findings of previous studies demonstrating an association between right hemisphere activation and increased narrative comprehension (George et al. 1999; Xu et al. 2005), as well as studies highlighting the inability of those with right hemisphere damage to comprehend text in a narrative context (Delis et al. 1983; Hough 1990). It also highlights the involvement of the right hemisphere in language comprehension, which may also support reading comprehension skill (as suggested by our DTI findings). This may provide a future neuroanatomical reference for differentiating children with reading difficulties (i.e., dyslexia) from children with reading comprehension problems (i.e., SLI) and may serve as an objective tool to evaluate the effectiveness of reading intervention programs on the technical reading vs reading comprehension domains.

Limitations of the study

The findings of the current study should be interpreted with several limitations in mind. First, differences between functional connectivity in ROIs in the right hemisphere vs the homologous ROIs in the left hemisphere did not reach significance, and therefore our conclusion of qualitatively greater right lateralization related to reading comprehension should be further examined. This fact poses a critical limitation to our conclusions of greater right structural and functional connectivity being related to better reading comprehension abilities. We suspect that in a larger or older group of children or adults that are more homogeneous in their reading level (i.e., 16–18 year olds or young adults), we might obtain more conclusive and powerful results as to the laterality of reading comprehension. In line with that, due to the relatively small group of children in this study, the results of our current DTI data did not reach significance after correction for multiple comparisons. Again, we suggest that a future study enrolling a larger number of participants may result in greater power and will survive multiple-comparisons correction. Secondly, although all children participating in the study reported intact reading, we did

Table 3 Weight of each network for the selected RO (seeds), for the functional connectivity analysis (sentence condition only), $P < 0.0005$, FDR-corrected. ROIs were defined using the Talairach-Daemon atlas in SPM 8

ROI-source	ROI Coordinates (x, y, z)	ROI-targets	F value	Beta Values	Intensity	# of targets in network
BA 20 (R)	53, -23, -31	BA 6 (R), BA 10 (R), BA 19 (L), BA 19 (R), BA 20 (L), BA 21 (R), BA 40 (R), BA 47 (R)	F(5)(18)=15.81	0.28	55.63	11
BA 21 (R)	64, -19, -17	BA 6 (R), BA 7 (L), BA 10 (L), BA 10 (R), BA 18 (L), BA 19 (L), BA 19 (R), BA 20 (L), BA 20 (R), BA 22 (L), BA 22 (R), BA 37 (L), BA 40 (R), BA 41 (L), BA 41 (R), BA 46 (R), BA 47 (R)	F(5)(18)=12.32	0.28	90.18	17
BA 19 (R)	35, -78, 19	BA 6 (R), BA 7 (L), BA 10 (R), BA 10 (L), BA 18 (L), BA 19 (L), BA 20 (L), BA 20 (R), BA 21 (R), BA 22 (L), BA 22 (R), BA 37 (L), BA 40 (R), BA 41 (L), BA 41 (R), BA 46 (R), BA 47 (R)	F(5)(18)=42.35	0.37	109.57	17
BA 40 (R)	56, -37, 42	BA 6 (R), BA 7 (L), BA 10 (R), BA 19 (L), BA 19 (R), BA 20 (L), BA 20 (R), BA 21 (R), BA 22 (L), BA 22 (R), BA 37 (L), BA 41 (L), BA 41 (R), BA 43 (R), BA 46 (R), BA 47 (R)	F(5)(18)=7.63	0.27	74.31	16
BA 43 (R)	64, -8, 13	BA 6 (R), BA 18 (L), BA 19 (L), BA 22 (L), BA 22 (R), BA 37 (L), BA 40 (R), BA 41 (L), BA 41 (R)	F(5)(18)=14.68	0.26	52.73	9
BA 47 (R)	39, 26, -20	BA 6 (R), BA 10 (R), BA 18 (L), BA 19 (L), BA 19 (R), BA 20 (L), BA 20 (R), BA 21 (R), BA 22 (L), BA 22 (R), BA 37 (L), BA 40 (R)	F(5)(18)=11.56	0.28	78.62	15
BA 46 (R)	54, 42, 8	BA 10 (L), BA 10 (R), BA 18 (L), BA 19 (L), BA 19 (R), BA 21 (R), BA 22 (L), BA 22 (R), BA 37 (L), BA 40 (R), BA 47 (R)	F(5)(18)=7.55	0.24	50.17	11
BA 6 (R)	32, 7, 50	BA 10 (L), BA 10 (R), BA 18 (L), BA 19 (L), BA 19 (R), BA 20 (L), BA 20 (R), BA 21 (R), BA 22 (L), BA 22 (R), BA 37 (L), BA 40 (R), BA 41 (L), BA 41 (R), BA 43 (R), BA 47 (R)	F(5)(18)=12.41	0.25	79.76	16
BA 10 (R)	26, 62, -4	BA 6 (R), BA 7 (L), BA 10 (L), BA 18 (L), BA 19 (L), BA 19 (R), BA 20 (L), BA 20 (R), BA 21 (R), BA 22 (L), BA 22 (R), BA 37 (L), BA 40 (R), BA 46 (R), BA 47 (R)	F(5)(18)=27.19	0.34	86.65	15
BA 22 (R)	62, -23, 3	BA 6 (R), BA 10 (L), BA 10 (R), BA 19 (L), BA 19 (R), BA 20 (L), BA 21 (R), BA 22 (L), BA 37 (L), BA 40 (R), BA 41 (R), BA 41 (L), BA 43 (R), BA 46 (R), BA 47 (R)	F(5)(18)=42.15	0.39	106.19	16
BA 41 (R)	51, -27, 10	BA 6 (R), BA 18 (L), BA 19 (L), BA 19 (R), BA 21 (R), BA 22 (L), BA 22 (R), BA 37 (L), BA 40 (R), BA 41 (L), BA 43 (R)	F(5)(18)=44.12	0.38	90.63	11
BA 10 (L)	-23, 62, -3	BA 6 (R), BA 7 (L), BA 10 (R), BA 18 (L), BA 19 (L), BA 19 (R), BA 20 (L), BA 20 (R), BA 21 (R), BA 22 (R), BA 37 (L), BA 46 (R), BA 47 (R)	F(5)(18)=20.75	0.31	73.20	13
BA 19 (L)	-31, -79, 20	BA 6 (R), BA 7 (L), BA 10 (L), BA 10 (R), BA 18 (L), BA 19 (R), BA 20 (L), BA 20 (R), BA 21 (R), BA 22 (L), BA 22 (R), BA 37 (L), BA 40 (R), BA 41 (R), BA 43 (R), BA 46 (R), BA 47 (R)	F(5)(18)=23.25	0.42	118.64	17
BA 18 (L)	-18, -90, 9	BA 6 (R), BA 10 (L), BA 10 (R), BA 19 (L), BA 19 (R), BA 21 (R), BA 22 (L), BA 22 (R), BA 37 (L), BA 41 (L), BA 41 (R), BA 43 (R), BA 46 (R), BA 47 (R)	F(5)(18)=21.17	0.32	88.88	14
BA 41 (L)	-47, -28, 12	BA 6 (R), BA 18 (L), BA 19 (R), BA 21 (R), BA 22 (L), BA 22 (R), BA 37 (L), BA 40 (R), BA 41 (R), BA 43 (R)	F(5)(18)=34.72	0.35	79.91	10
BA 20 (L)	-51, -23, -29	BA 6 (R), BA 7 (L), BA 10 (L), BA 10 (R), BA 19 (L), BA 19 (R), BA 20 (R), BA 21 (R), BA 22 (R), BA 37 (L), BA 40 (R), BA 47 (R)	F(5)(18)=13.49	0.77	61.77	12
BA 22 (L)	-59, -25, 5	BA 6 (R), BA 10 (R), BA 18 (L), BA 19 (L), BA 19 (R), BA 21 (R), BA 22 (R), BA 37 (L), BA 40 (R), BA 41 (L), BA 41 (R), BA 43 (R), BA 46 (R), BA 47 (R)	F(5)(18)=40.31	0.42	100.31	14
BA 7 (L)	-15, -58, 55	BA 10 (L), BA 10 (R), BA 18 (L), BA 19 (L), BA 19 (R), BA 20 (L), BA 37 (L), BA 40 (R), BA 47 (R)	F(5)(18)=11.58	0.24	52.09	9
BA 37 (L)	-49, -57, -7	BA 6 (R), BA 7 (L), BA 10 (L), BA 10 (R), BA 19 (L), BA 19 (R), BA 20 (L), BA 20 (R), BA 21 (R), BA 22 (L), BA 22 (R), BA 40 (R), BA 41 (L), BA 41 (R), BA 43 (R), BA 46 (R), BA 47 (R)	F(5)(18)=41.66	0.38	111.92	18

not assess the technical reading of our participants, so we cannot demonstrate the distinct role of the right hemisphere in reading comprehension in these children. Third, when including a priori ROIs in an analysis such as those we included in the functional connectivity analysis (and also in the structural connectivity analysis using DTI) that is the same limitation

for every hypothesis (ROI)-driven analysis, may lose important information regarding other regions that are involved in the process, but were not included in the analysis. An alternative approach would be to perform the functional connectivity analysis first and then choose the white matter tracts corresponding with these regions for the structural connectivity

correlation with the percentiles for the Passage Comprehension task.

Acknowledgments Data presented in this work was obtained from the database provided by the Pediatric Functional Neuroimaging Research Network known as Cincinnati MR Imaging of Neuro-Development (CMIND) at <https://research.cchmc.org/c-mind/>. This Network and the resulting CMIND database were supported by a contract from the Eunice Kennedy Shriver National Institute of Child Health and Human Development (HHSN275200900018C). The authors thank J. Denise Wetzel, CCHMC Medical Writer, for editing of the manuscript.

Conflict of interest Tzipi Horowitz-Kraus, Molly Grainger, Mark DiFrancesco, Jennifer Vannest, Scott K. Holland, and the CMIND Authorship Consortium (Holland, Vannest, Schmithorst, Altaye, Lee, Hernandez-Garcia, Wagner, Toga, Levitt, Byars, Dimitrijevic, Felicelli, Kadis, Leach, Peariso, Plante, Rajagopal, Rupert, Schapiro, Ly, Petrosyan, Wang, and Freund) declare that they have no conflicts of interest.

Informed consent All procedures followed were in accordance with the ethical standards of the responsible committee on human experimentation (institutional and national) and with the Helsinki Declaration of 1975, and the applicable revisions at the time of the investigation. Informed consent was obtained from all patients for being included in the study.

References

- Avants, B. B., Epstein, C. L., Grossman, M., & Gee, J. C. (2008). Symmetric diffeomorphic image registration with cross-correlation: evaluating automated labeling of elderly and neurodegenerative brain. *Medical Image Analysis*, *12*(1), 26–41.
- Behrens, T. E., Woolrich, M. W., Jenkinson, M., Johansen-Berg, H., Nunes, R. G., Clare, S., et al. (2003). Characterization and propagation of uncertainty in diffusion-weighted MR imaging. *Magnetic Resonance Medicine*, *50*(5), 1077–1088.
- Benjamini, Y., & Hochberg, Y. (1995). Controlling for the false discovery rate: a practical powerful approach to multiple testing. *Journal of Royal Statistical Society*, *57*(1), 289–300.
- Booth, J. R., MacWhinney, B., Thulborn, K. R., Sacco, K., Voyvodic, J., & Feldman, H. M. (1999). Functional organization of activation patterns in children: whole brain fMRI imaging during three different cognitive tasks. *Progress in Neuropsychopharmacology Biological Psychiatry*, *23*, 669–682.
- Byars, A., Holland, S., Strawsburg, R., Bommer, W., Dunn, S., Schmithorst, V., et al. (2002). Practical aspects of conducting large-scale functional magnetic resonance imaging studies in children. *Journal of Child Neurology*, *17*, 885–889.
- Caplan, D., Vijayan, S., Kuperberh, G., West, C., Waters, G., Greve, D., et al. (2001). Vascular responses to syntactic processing: event-related fMRI study of relative clauses. *Human Brain Mapping*, *15*, 26–38.
- Chall, J. (1983). *Stages of reading development*. New York: McGraw-Hill.
- Cutting, L. E., Clements, A. M., Courtney, S., Rimrod, S. R., Schafer, J. G. B., Wilkins, J., et al. (2006). Differential components of sentence comprehension: beyond single word reading and memory. *NeuroImage*, *29*, 429–438.
- Delis, D. C., Wapner, W., Gardner, H., & Moses, J. A. (1983). The contribution of the right hemisphere to the organization of paragraphs. *Cortex*, *19*, 43–50.
- Friederici, A. (2009). Pathways to language: fiber tracts in the human brain. *Trends in Cognitive Sciences*, *13*(4), 175–181.
- Friederici, A. (2012). The cortical language circuit: from auditory perception to sentence comprehension. *Trends in Cognitive Science*, *16*, 262–268.
- Friederici, A., Rüschemeyer, S., Hahne, A., & Fiebach, C. (2003). The role of the left inferior frontal and superior temporal cortex in sentence comprehension: Localizing syntactic and semantic processes. *Cerebral Cortex*, *13*(2), 170–177.
- Friederici, A. D., Fiebach, C. J., Schlesewsky, M., Bornkessel, I. D., & von Cramon, D. Y. (2006). Processing linguistic complexity and grammaticality in the left frontal cortex. *Cerebral Cortex*, *16*, 1709–1717.
- George, M., Kutas, M., Martinez, A., & Sereno, M. I. (1999). Semantic integration in reading: engagement of the right hemisphere during discourse processing. *Brain*, *122*, 1317–1325.
- Gough, P. B., & Tunmer, W. E. (1986). Decoding, reading, and reading disability. *Remedial and Special Education*, *7*, 6–10.
- Horowitz-Kraus, T., Vannest, J. J., & Holland, S. K. (2013). Overlapping neural circuitry for narrative comprehension and proficient reading in children and adolescents. *Neuropsychologia*, *51*, 2651–2662.
- Horowitz-Kraus, T., Wang, Y. Y., Plante, E., & Holland, S. K. (2014). The involvement of the right hemisphere in reading comprehension: a DTI study. *Brain Research*. doi:10.1016/j.brainres.2014.05.034.
- Hough, M. S. (1990). Narrative comprehension in adults with right and left hemisphere brain damage: theme organization. *Brain and Language*, *38*, 253–77.
- Jenkinson, M., Bannister, P., Brady, M., & Smith, S. (2002). Improved optimization for the robust and accurate linear registration and motion correction of brain images. *Neuroimage*, *17*(2), 825–841.
- Johns, C. L., Tooley, K. M., & Traxler, M. J. (2008). Discourse impairments following right hemisphere brain damage: a critical review. *Language and Linguistics Compass*, *2*, 1038–1062.
- Keller, T. A., Carpenter, P. A., & Just, M. A. (2003). Brain imaging of tongue-twister sentence comprehension: twisting the tongue and the brain. *Brain and Language*, *84*, 189–203.
- Mason, R. A., & Just, M. A. (2007). Lexical ambiguity in sentence comprehension. *Brain Research*, *1146*, 115–127.
- Meyer, M., Friederici, A. D., & von Cramon, D. Y. (2000). Neurocognition of auditory sentence comprehension: event related fMRI reveals sensitivity to syntactic violations and task demands. *Cognitive Brain Research*, *9*, 19–33.
- Muller, O., & Hagoort, P. (2006). Access to lexical information in language comprehension: semantic before syntax. *Journal of Cognitive Neuroscience*, *18*(1), 84–96.
- Nation, K., & Snowling, M. (1997). Assessing reading difficulties: the validity and utility of current measures of reading skill. *British Journal of Educational Psychology*, *67*, 359–370.
- Ni, W., Constable, R. T., Mencl, W. E., Pugh, K. R., Fulbright, R. K., & Shaywitz, S. E. (2000). An event-related neuroimaging study distinguishing form and content in sentence processing. *Journal of Cognitive Neuroscience*, *12*, 120–133.
- Nichols, T., & Holmes, A. (2002). Nonparametric permutation tests of functional neuroimaging: a primer with examples. *Human Brain Mapping*, *15*(1), 1–25.
- Plante, E., Ramage, A. E., & Magloire, J. (2006). Processing narratives for verbatim and gist information by adults with language learning disabilities: A functional neuroimaging study. *Learning Disabilities Research & Practice*, *21*, 61–76.
- Rimrod, S. L., Clements-Stephens, A. M., Pugh, K. R., Courtney, S. M., Gaur, P., Pekar, J. J., et al. (2009). Functional MRI of sentence comprehension in children with dyslexia: beyond word recognition. *Cerebral Cortex*, *19*, 402–413.
- Robertson, D. A., Gernsbacher, M. A., Guidotti, S. J., Robertson, R. R. W., Irwin, W., Mock, B. J., et al. (2000). Functional neuroanatomy of the cognitive processes of mapping during discourse comprehension. *Psychological Science*, *11*, 255–260.

- Roman, M., Brownell, H. H., Potter, H. H., & Seibold, M. S. (1987). Script knowledge in right hemisphere-damaged and in normal elderly adults. *Brain and Language*, *31*, 151–170.
- Schmithorst, V. J., Hernandez-Garcia, L., Vannest, J., Rajagopal, A., Lee, G., & Holland, S. K. (2014). Optimized simultaneous ASL and BOLD functional imaging of the whole brain. *Journal of Magnetic Resonance Imaging*, *39*(5), 1104–1117. doi:10.1002/jmri.24273.
- Smith, S. M., Jenkinson, M., Johansen-Berg, H., Rueckert, D., Nichols, T. E., Mackay, C. E., et al. (2006). Tract-based spatial statistics: Voxelwise analysis of multi-subject diffusion data. *NeuroImage*, *31*(4), 1487–1505.
- Smith, S. M., Johansen-Berg, H., Jenkinson, M., Rueckert, D., Nichols, T. E., Miller, K. L., et al. (2007). Acquisition and voxelwise analysis of multi-subject diffusion data with Tract-Based Spatial Statistics. *Nature Protocols*, *2*, 499–503.
- Spencer, M., Quinn, J., & Wagner, R. (2014). Specific reading comprehension disability: major problem, myth, or misnomer? *Learning Disabilities Research & Practice*, *29*(1), 3–9.
- Stothard, S., & Hulme, C. (1995). A comparison of phonological skills in children with reading comprehension difficulties and children with decoding difficulties. *Journal of Child Psychology and Psychiatry*, *36*(3), 399–408.
- Su, P., Kuan, C. C., Kaga, K., Sano, M., & Mima, K. (2008). Myelination progression in language-related regions in brain of normal children determined by quantitative MRI assessment. *International Journal of Pediatric Otorhinolaryngology*, *72*(12), 1751–1763.
- Torgesen, J. K., Wagner, R. K., & Rashotte, C. A. (2012). *Test of word reading efficiency (TOWRE)*. Austin: Pro-Ed.
- Turkeltaub, P. E., Gareau, L., Flowers, D. L., Zeffiro, T. A., & Eden, G. F. (2003). Development of neural mechanisms for reading. *Nature Neuroscience*, *6*, 767–773.
- Vogel, A. C., Petersen, S. E., & Schlaggar, B. L. (2014). The VWFA: it's not just for words anymore. *Frontiers in Human Neuroscience*, *8*, 1–10.
- Wang, Y., Adamson, C., Yuan, W., Altaye, M., Rajagopal, A., Byars, A. W., et al. (2012). Sex differences in white matter development during adolescence: a DTI study. *Brain Research*, *1478*, 1–15.
- Wapner, W., Hamby, S., & Gardner, H. (1981). The role of the right hemisphere in the apprehension of complex linguistic materials. *Brain and Language*, *14*, 15–33.
- Wechsler, D. (2003). *Wechsler Intelligence Scale for Children- WISC-IV*. Psychological Corporation.
- Whitfield-Gabrieli, S., & Nieto-Castanon, A. (2012). Conn: A functional connectivity toolbox for correlated and anti-correlated brain networks. *Brain Connectivity*, *2*(3), 125–141.
- Wilke, M., Schmithorst, V., & Holland, S. K. (2003). Normative pediatric brain data for spatial normalization and segmentation differs from standard adult data. *Magnetic Resonance Medicine*, *50*(4), 749–757.
- Woodcock, R., McGrew, K. S., & Mather, N. (2001). *Woodcock-Johnson psycho-educational battery-third edition*. Itasca: Riverside Publishing.
- Xu, J., Kemeny, S., Park, G., Frattali, C., & Braun, A. (2005). Language in context: emergent features of word, sentence, and narrative comprehension. *NeuroImage*, *25*(3), 1002–1015.
- Yeatman, J., Dougherty, R., Ben-Shachar, M., & Wandell, B. (2012). Development of white matter and reading skills. *Proceedings of the National Academy of Sciences of the United States of America*, *109*(44), E3045–E3053.
- Yuill, N., & Oakhill, J. (1991). *Children's problems in text comprehension: An experimental investigation*. Cambridge University Press.